# Practical applications of global optimisation techniques in 2-D resistivity inversion

M.H. Loke[1], A. Vinciguerra[2], P.B. Wilkinson[3], A. Hojat[4]

[1] Geotomo Software Sdn Bhd; [2] Université de Strasbourg; [3] British Geological Survey; [4] Politecnico di Milano

## Summary

The data collected from 2-D ERT surveys is usually inverted using a nonlinear local optimisation method such as the smoothness-constrained least-squares method. This method attempts to find the minimum of an objective function that consists of the data misfit and model roughness. The least-squares method converges rapidly to a minimum but it might be a non-optimal local minimum. A global optimisation method can locate the optimal global minimum but the calculation time increases exponentially with the number of parameters. A global optimisation method (simulated annealing) is used refine the model obtained by the least-squares method at the regularisation parameter value found by the L-curve method. Inversion of a data set from a 2-D survey over a levee at Colorno (Italy) shows that the simulated annealing method does locate an objective function minimum that is consistently lower than that found the least-squares method. Although the maximum difference is usually less than 10%, the refinement step serves as a check on the model found by the least-squares method. A method to estimate the optimum regularisation parameter using a best fitting analytic function to the numerical L-curve points where conventional methods might give ambiguous results is presented.

# Practical applications of global optimisation techniques in 2-D resistivity inversion

## Introduction

The data collected from 2-D and 3-D geoelectrical surveys, particularly in commercial surveys, are usually inverted using a local optimisation method to produce a subsurface resistivity model. The optimisation method attempts to find the minimum of an objective function that consists of the data misfit and selected model constraints. The objective function can be written as

$$P(\mathbf{y},\mathbf{q}) = \varphi(\mathbf{y}) + \lambda\phi(\mathbf{q}) . \qquad (1)$$

$P(\mathbf{y},\mathbf{q})$ is the objective function, $\varphi(\mathbf{y})$ is the data misfit (difference between the logarithms of the measured and calculated apparent resistivity values) and $\phi(\mathbf{q})$ is the model roughness. $\mathbf{y}$ and $\mathbf{q}$ represent the data values and model parameters. The regularisation parameter $\lambda$ is the weight given to minimizing $\phi(\mathbf{q})$ compared to $\varphi(\mathbf{y})$. The optimisation method attempts to find the set of model parameters $\mathbf{q}$ at the minimum of the objective function $P$ (Oldenburg and Li, 2005). The data values in 2-D ERT surveys are the apparent resistivity values and the positions of the electrodes, while the model parameters are the subsurface resistivity values. A 2-D model that consists of hundreds of cells (thousands in 3-D) is used so that complex variations in the subsurface resistivity can be accurately modelled. There are two related practical problems in solving equation (1) to obtain the model $\mathbf{q}$. The first problem is finding the optimum value for the regularisation parameter $\lambda$, while the second is to determine the model parameters $\mathbf{q}$. There are two main classes of numerical methods to obtain model parameters starting from a given model (such as a homogenous half-space), local and global optimisation methods. Many local optimisation methods use the gradient of the objective function (the Jacobian matrix) to find a new model at a lower value of the objective function. One such method is the smoothness-constrained least-squares method (Oldenburg and Li, 2005). This method is widely used for the inversion of data from 2-D and 3-D surveys which can have hundreds of thousands of data points and model parameters (Loke *et al.*, 2020). It converges rapidly but can become trapped in a non-optimal local minimum (Sen and Stoffa, 2013; Aleardi *et al.*, 2019). Global optimisation methods attempt to find the optimal global minimum but the calculation time increases exponentially with the number of model parameters. They are widely used in the inversion of 1-D models with a small number of parameters (Su *et al.*, 2023). To reduce the number of parameters for 2-D and 3-D inversion, one approach is to use simple geometric models such as a rectangular block or prism embedded in a homogeneous medium (Shamara *et al.*, 2023). However, these simple models cannot accurately model the complex resistivity variations encountered in field surveys and often have data misfits of over 100%. Most commercial ERT surveys are carried out by small geophysical companies with a limited budget and computational facilities (usually a PC). This paper is focussed on practical techniques which can be used by such companies.

## Theory and Method

The smoothness-constrained least-squares method determines the model parameters $\mathbf{q}$ (logarithm of model resistivity) by solving the following equation in an iterative manner.

$$\left(\boldsymbol{J}^T \boldsymbol{R}_d \boldsymbol{J} \quad + \lambda \boldsymbol{F}_R\right)\boldsymbol{\Delta q}_k = \boldsymbol{J}^T \boldsymbol{R}_d \boldsymbol{g} \quad - \lambda(\boldsymbol{F}_R + \alpha \boldsymbol{I})(\boldsymbol{q}_k - \boldsymbol{q}_R) \qquad (2)$$

where $\boldsymbol{F}_R = \boldsymbol{C}_x^T \boldsymbol{R}_{mx} \boldsymbol{C}_x + \boldsymbol{C}_y^T \boldsymbol{R}_{my} \boldsymbol{C}_y + \boldsymbol{C}_z^T \boldsymbol{R}_{mz} \boldsymbol{C}_z$

$\boldsymbol{q}_k$ is the model for the $k$th iteration and $\Delta\mathbf{q}_k$ is the change in the model required to reduce the data misfit $\boldsymbol{g}$. $\boldsymbol{q}_R$ is a reference model (usually the average of the measured apparent resistivity values). $\mathbf{C}_x$, $\mathbf{C}_y$ and $\boldsymbol{C}_z$ are the roughness filter matrices in the $x$-, $y$- and $z$-directions to minimise changes in the model resistivity values. $\boldsymbol{R}_d$ and $\boldsymbol{R}_m$ are weighting matrices for the data misfit and model roughness vectors. $\alpha$ is a regularisation factor to reduce the model deviation from a reference model. $\boldsymbol{J}$ is the Jacobian matrix. A slow cooling sequence where the regularisation parameter $\lambda$ is gradually reduced with each iteration (Oldenburg and Li, 2005) is commonly used. The objective function depends on the regularisation parameter $\lambda$. A value which is too large will result in a model with small changes in the resistivity values (low model roughness) but a high data misfit. A value that is too small will result in a model with excessive structure (high model roughness) and low data misfit. Thus, an important first step is to estimate the optimum regularisation parameter which is dependent on the noise level in the measured data and the subsurface resistivity variations. Farquharson and Oldenburg (2004) described two methods to estimate the optimum damping factor, the Generalized Cross Validation (GCV) and L-curve methods. The GVC method is impractical to use for large 2-D and 3-D problems as it requires the inverse of a *m-by-m* matrix which requires about $m^3$ operations (*m* is the number of model parameters). Thus, the L-curve method is used in this research. The L-curve for a field data set is determined by carrying an inversion of the data set using a range of regularisation values. The optimum value is given by the point with the maximum curvature (Farquharson and Oldenburg, 2004; Loke *et al.*, 2022).

**Example**

The data set from a 2-D ERT survey using the Wenner array with 48 electrodes and a 2-metre spacing over a levee in Colorno, Italy (Hojat, 2024) is used as an example. The data set has 360 measurements (Figure 1a). The survey was part of a long-term experiment to monitor changes within and below the levee such as seepages. The processing of this data set was done in 2 steps (1) finding the optimum regularisation parameter using the least-squares method, and (2) refining the model using a global optimisation method.

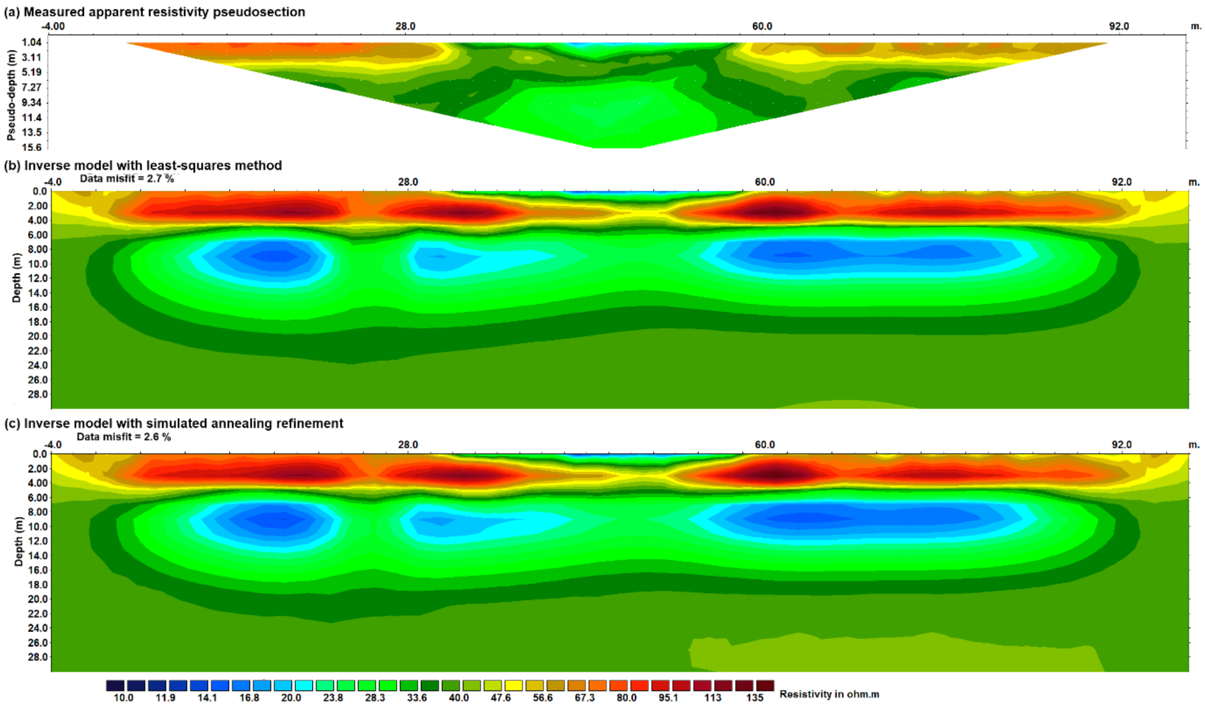


***Figure 1*** *Colornos levee survey. (a) Measured apparent resistivity pseudosection. (b) Inverse model with least-squares method. (c) inverse model with simulated annealing refinement step.*

The inverse model grid used is extended by 4 metres at both ends of the line to reduce artefacts due to structures outside the line (Maurer and Friedel, 2006). It has 15 layers and 565 model cells. The least-squares method first is used to find the models obtained from a high value (0.15) to a low value (0.00015) of the regularisation parameter $\lambda$. The L-curve plot is shown in Figure 2a. The calculation time taken using a PC with a 16-core Intel 12900K CPU was 10 seconds. The curvature plot (Figure 2b) has a maximum point corresponding to a $\lambda$ value of 0.00311. The inverse model is shown in Figure 1b. The least-squares inverse model was then used as the starting model for the simulated annealing method (Press *et al.*, 2007). Figure 1c shows the model obtained by the simulated annealing method which took 9248 seconds. The simulated annealing refinement step reduced the objective function from 0.673 to 0.652. There are small differences between the simulated annealing (Figure 1c) and the least-squares models (Figure 1b). However, the differences are not large enough to change a geological interpretation of the results. The calculation time taken for the simulated annealing model was 9248 seconds which is nearly 1000 times higher than the least-squares method, but still practical with present day PCs for 2-D inversions. The procedure used in this paper first carries out an inversion of the data using the least-squares method for a large range of $\lambda$ values to determine the optimum value using the L-curve method. Then another inversion is carried out using the least-squares method up to the optimum

$\lambda$ value followed by a refinement step using a global optimisation method. This will check whether the local optimisation nature of the least-squares method has a significant effect on the results. Figure 2c shows the change in the objective function value for the entire range of $\lambda$ used by both methods. The objective function value achieved by the simulated annealing method is consistently lower but the gap becomes narrower as the $\lambda$ decreases. The maximum difference is about 9%.

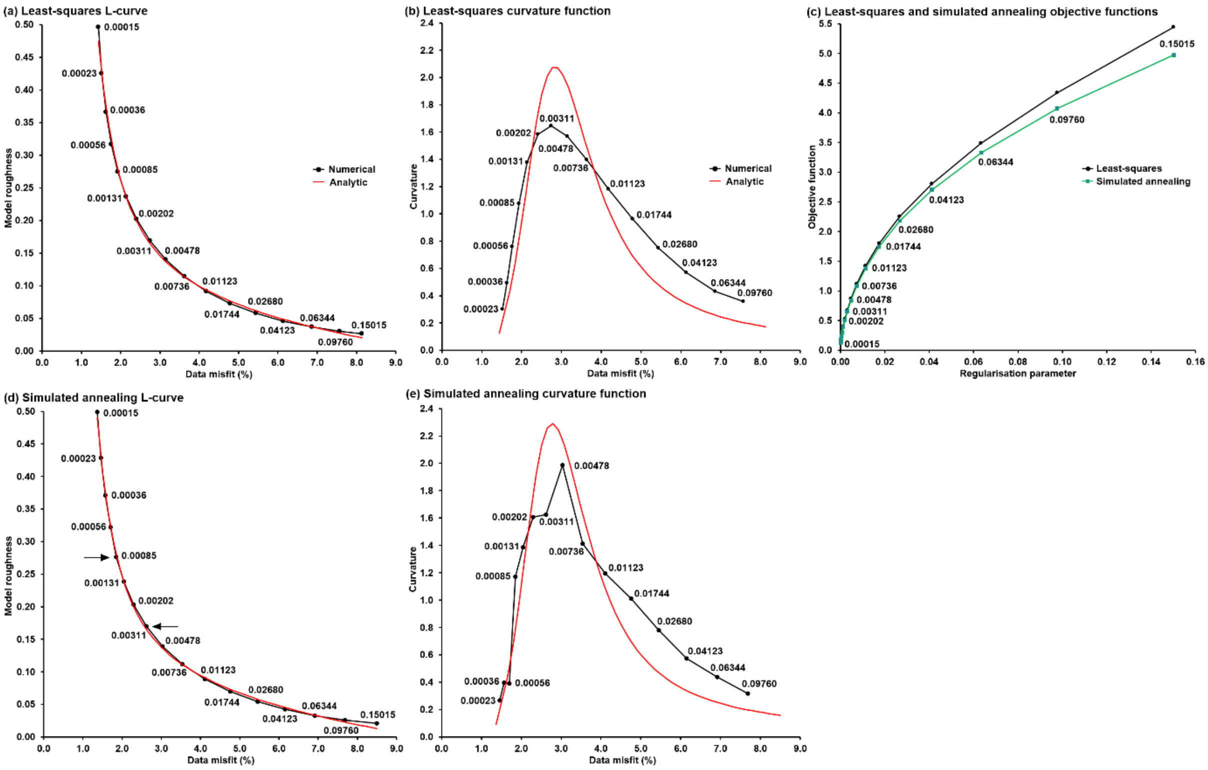


***Figure 2** (a) L-curve plot for the inversion of the Colornos levee data set using the least-squares method and (b) its curvature. (c) Change of the objective function with the least-squares and simulated annealing methods. (d) L-curve with simulated annealing refinement step and (e) curvature plot. The regularisation parameter value $\lambda$ is shown next to the points on the curves.*

Figures 2d and 2e show the L-curve plots for the simulated annealing models. Figure 2e shows a practical problem with the use of the L-curve method for field data sets. Gunther *et al.* (2006) observed that it does not always provide a satisfactory solution. The curvature values calculated using the second order derivative of the L-curve are very sensitive to small deviations from a smooth curve (Figure 2e), such as the points corresponding to $\lambda$ values of 0.00311 and 0.00085 (Figure 2d). This causes the curvature values near these points to deviate significantly from an ideal L-curve. For some field data sets, the deviations from an ideal L-curve can be much larger making the identification of the maximum curvature point difficult (Loke, 2025). The shape of the L-curve is affected by noise in the data, which could be due to random geoelectrical noise or errors in the positions of the electrodes (Loke *et al.*, 2020, 2022). One possible solution is to find a best fitting analytic function for the observed data misfit-model roughness points (red curves in Figures 2a and 2d). The curvature of the analytic function can then be calculated to estimate the maximum point (Figures 2b and 2e). The function used has the following form with seven parameters *a*, *b*, *c*, *d*, *e*, *f* and *g* that are numerically determined using the least-squares optimisation method (Lines and Treitel, 1984).

$$y = a.\left(\frac{e}{x}\right)^{f} + b.\left(\frac{e}{x}\right)^{f/2} + c.\left(\frac{e}{x}\right)^{f/3} + d.\left(\frac{e}{x}\right)^{f/4} + g \quad (3)$$

This function is similar to a Taylor series expansion. Tests were conducted using different number of terms in the series. Adding the second term made a large improvement compared to using the first term alone. Adding the third term made a significant improvement, while adding the fourth term gave a smaller improvement. The curvature of the analytic function (Figure 2b) has a maximum near the numerically calculated $\lambda$ value of 0.00311. This function gives a reasonable fit for most data sets near the corner of the L-curve but a poorer fit at the ends for small or large $\lambda$ values.

**Conclusions**

The objective function value obtained using the least-squares method can be further reduced by using a simulated annealing refinement step. A method using a best-fitting analytic function for the numerical L-curve to estimate the optimum regularisation parameter is presented for noisy data sets where conventional methods might give ambiguous results. Research is being conducted to reduce the calculation time by using more sophisticated global optimisation methods such as very fast simulated annealing (Ingber, 1989), PSO (Su *et al.*, 2019) and MCMC (Vinciguerra *et al.*, 2022). We are also examining an alternative algorithm that starts with the global optimisation method and a homogeneous half-space model to locate the approximate region with the minimum followed by the least-squares method.

**Acknowledgements**

Wilkinson publishes with the permission of the Executive Director of the British Geological Survey.

**References**

Aleardi, M., Pierini, S. and Sajeva, A. [2019]. Assessing the performances of recent global search algorithms using analytic objective functions and seismic optimization problems. *Geophysics*, **84**(5), 1SO-Z28

Farquharson, C.G., and Oldenburg, D.W. [2004]. A comparison of automatic techniques for estimating the regularization parameter in non-linear inverse problems. *Geophysical Journal International*, **156**, 411-425.

Gunther, T., Rucker, C. and Spitzer, K. [2006]. Three-dimensional modelling and inversion of dc resistivity data incorporating topography – II. Inversion. *Geophysical Journal International*, **166**, 506–517.

Hojat, A. [2024] An iterative 3D correction plus 2D inversion procedure to remove 3D effects from 2D ERT data along embankments. Sensors **24**(12), 3759, https://doi.org/10.3390/s24123759.

Ingber, L. [1989]. Very fast simulated re-annealing. *Mathematical and Computer Modelling*, **12**(8), 967-973.

Lines L.R. and Treitel S. [1984]. Tutorial: A review of least-squares inversion and its application to geophysical problems. *Geophysical Prospecting*, **32**, 159-186.

Loke, M.H., Papadopoulos, N, Wilkinson, P.B., Oikonomou, D., Simyrdanis, K. and Rucker, D. [2020]. The inversion of data from very large 3-D ERT mobile surveys. *Geophysical Prospecting*, **68**, 2579-2597.

Loke, M.H., Wilkinson, P.B., Chambers, J.E., Uhlemann, S., Dijkstra, T. and Dahlin, T. [2022]. The use of asymmetric time constraints in 4-D ERT inversion. *Journal of Applied Geophysics*, **197**, 104536.

Loke, M.H. [2025]. Tutorial : 2-D and 3-D electrical imaging surveys. Geotomo Software (www.geotomosoft.com).

Maurer, H. and Friedel, S. [2006]. Outer-space sensitivities in geoelectrical tomography. *Geophysics*, **71**, 1942-2156.

Oldenburg, D.W. and Li, Y. [2005]. *5. Inversion for Applied Geophysics: A Tutorial. Near-Surface Geophysics (SEG Investigations in Geophysics Series No. 13)*, 89-150.

Press, W.H., Teukolsky S.A., Vetterling W.T. and Flannery B.P. [2007]. *Numerical Recipes in C (Third Edition)*. Cambridge University Press, U.K.

Sen, M.K. and Stoffa, P.L. [2013]. *Global Optimization Methods in Geophysical Inversion*. Cambridge University Press, U.K.

Shamara, Z., C.-A., Leticia, F.-M.E., Andrés, T.-A., Adrián, M., L.-M. and René E., C.-S. [2023]. Inversion of ERT-3D data using PSO and weighting functions. *Journal of Applied Geophysics*, **215**, 105091.

Vinciguerra, A., Aleardi, M., Hojat, A, Loke, M.H. and Stucchi, E. [2022]. Discrete Cosine Transform for Parameter Space Reduction in Bayesian Electrical Resistivity Tomography. *Geophysical Prospecting*, **70**, 193-209.

Su, P., Yang, J. and Xu, L. [2023]. 1D regularization inversion combining particle swarm optimization and least squares method. *Applied Geophysics*, **20**, 77–87.